

# Thioether-ligated nickel(I) complexes for the activation of dioxygen †

Koyu Fujita, Arnold L. Rheingold and Charles G. Riordan\*

Department of Chemistry and Biochemistry, University of Delaware, Newark, DE 19716, USA.

E-mail: riordan@udel.edu

Received 11th December 2002, Accepted 16th January 2003

First published as an Advance Article on the web 23rd April 2003

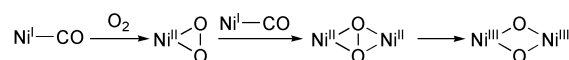
The preparation of phenyltris[1-adamantyl(thiomethyl)]borate [PhTt<sup>Ad</sup>], which incorporates the large 1-adamantyl thioether substituent, is described. This derivative was sought to permit the preparation of four-coordinate nickel(I) complexes. Following a synthetic scheme for the related *tert*-butyl ligand, [PhTt<sup>Bu</sup>], the following complexes were prepared and characterized fully, [PhTt<sup>Ad</sup>]Ni(CO), [PhTt<sup>Ad</sup>]Ni(PMe<sub>3</sub>) and [κ<sup>2</sup>-PhTt<sup>Ad</sup>]Ni(η<sup>2</sup>-CH<sub>2</sub>SAd). The last species is a degradation product resulting from attempted reduction of the nickel(II) precursor, [PhTt<sup>Ad</sup>]NiCl, in the absence of a ligand suitable for trapping the nickel(I) fragment.

## Introduction

Previous studies from this laboratory established that nickel(I) complexes<sup>1,2</sup> supported by the thioether ligand, phenyltris[*tert*-butyl(thiomethyl)]borate (abbreviated [PhTt<sup>Bu</sup>]), upon low temperature exposure to dioxygen generated the thermally sensitive bis-μ-oxo dimer, [(PhTt<sup>Bu</sup>)Ni]<sub>2</sub>(μ-O)<sub>2</sub>, Scheme 1.<sup>3</sup> The purple dimer was identified by a variety of spectroscopic methods, most conclusively by resonance Raman and EXAFS studies.<sup>4</sup> A low energy Ni–O stretching mode at 590 cm<sup>-1</sup> displayed an <sup>18</sup>O isotope sensitivity (shifting to 560 cm<sup>-1</sup>) similar to other bis-μ-oxo complexes. The resonance excitation profile of this mode correlated with an intense optical absorption band at 565 nm ascribed to an oxo → nickel(III) charge transfer transition.<sup>5</sup> Nickel EXAFS analysis supported the molecular structure assignment, showing short Ni–O distances at 1.82 Å and a Ni–Ni vector at 2.83 Å. The latter attribute is a definitive characteristic of such “diamond core” structures.<sup>4</sup> While other nickel bis-μ-oxo dimers supported with nitrogen donors have been described, their preparations result from hydrogen peroxide oxidation of dinuclear nickel(II) precursors.<sup>6–9</sup> Given the opportunity to explore the composition and reactivity of dioxygen-derived intermediates provided by our initial observation, we have embarked on a program to

define the landscape of reactions between nickel(I) and dioxygen.

To elucidate the mechanism of formation of [(PhTt<sup>Bu</sup>)Ni]<sub>2</sub>(μ-O)<sub>2</sub> from its nickel(I) precursor and dioxygen, we began by considering the series of elementary steps below.

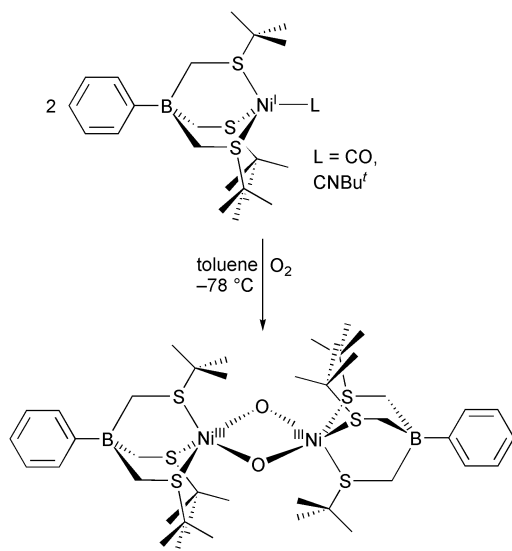


An analogous scheme has been proposed, and supported with a great wealth of experimental evidence, for the activation of dioxygen by copper complexes.<sup>10–13</sup> Presuming that 1 : 1 adduct formation precedes dimer production, we aimed to modify the [PhTt<sup>Bu</sup>] ligand so as to preclude access to dinuclear structures thus stabilizing such an adduct allowing for its identification. Given that the *tert*-butyl substituents were ineffective in preventing dimer formation, the larger 1-adamantyl groups were deemed appropriate in that they would yield nickel(I) complexes of appropriate electronic structure to activate dioxygen. This paper describes the preparation of the new ligand, [PhTt<sup>Ad</sup>], and the nickel(II) and nickel(I) precursors necessary to explore nickel–dioxygen reactivity with the goal of stabilizing a 1 : 1 adduct.

## Results and discussion

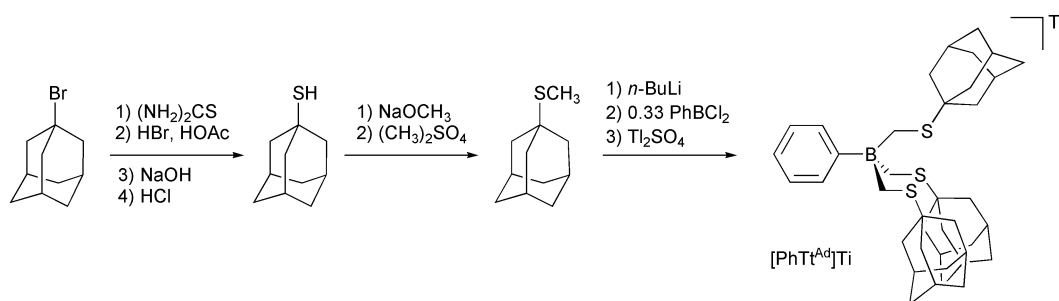
### Ligand synthesis

The preparation of the [PhTt<sup>Ad</sup>]Tl ligand, as outlined in Scheme 2, initiates from the commercially available 1-bromoadamantane as 1-adamantane thiol is not readily available. Reaction with thiourea under the acidic conditions of HBr and AcOH, followed by addition of base and neutralization produced 1-adamantane thiol in 65% yield. 1-Adamantane methyl sulfide was generated in high yield following the deprotonation and subsequent methylation of 1-adamantane thiol.<sup>14</sup> This procedure follows that detailed previously for *tert*-butyl methyl sulfide.<sup>15,16</sup> Given the lower volatility of 1-adamantane thiol compared with *tert*-butyl thiol, no special precautions are necessary to avoid liberating noxious mercaptan odors. Conversion of 1-adamantane methyl sulfide to the ligand [PhTt<sup>Ad</sup>] was accomplished as for the other ligands in this class.<sup>17–19</sup> For stability and solubility purposes, [PhTt<sup>Ad</sup>] was precipitated from aqueous solution as its thallium(I) salt. The material is a white, microcrystalline solid, stable in air and soluble in a range of common organic solvents. The solid state structure of [PhTt<sup>Ad</sup>]Tl, elucidated by X-ray diffraction, consists of a one-dimensional extended chain of alternating cations and anions. In the lattice each Tl<sup>+</sup> is coordinated to three sulfurs,



Scheme 1

† Based on the presentation given at Dalton Discussion No. 5, 10–12th April 2003, Noordwijkerhout, The Netherlands.



Scheme 2

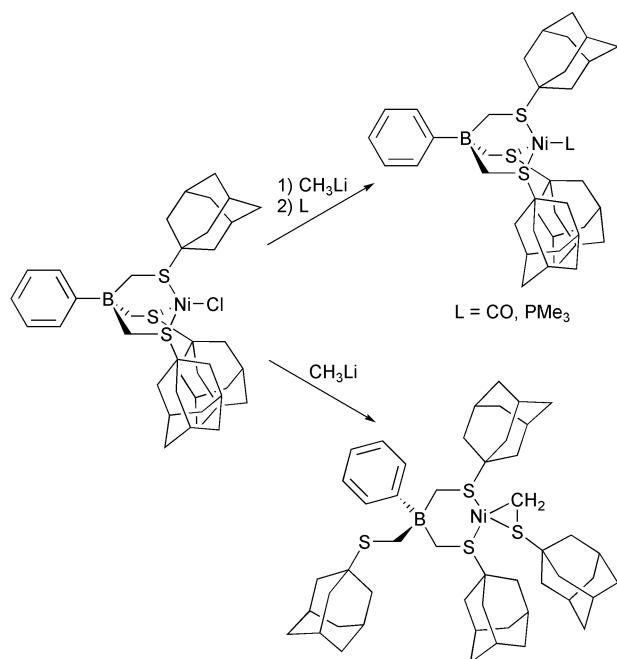
two from one  $[\text{PhTt}^{\text{Ad}}]$  ligand and the third from an adjacent  $[\text{PhTt}^{\text{Ad}}]$ . Furthermore, the borato ligand providing one thioether is interacting with the metal ion *via* an  $\eta^6\text{-PhB}$  mode.

### Nickel complex synthesis

The targeted starting synthon for these studies,  $[\text{PhTt}^{\text{Ad}}]\text{NiCl}$ , was prepared *via* the metathetical reaction of  $[\text{PhTt}^{\text{Ad}}]\text{Ti}$  and  $\text{NiCl}_2 \cdot 6\text{H}_2\text{O}$  in methanol–chloroform. The deep brick-red solid is stable to air and moisture and freely soluble in a range of solvents including THF and chlorinated hydrocarbons. Its electronic and NMR spectral characteristics (Experimental) are consistent with three-fold coordination of the borato ligand yielding a  $T_d$  nickel complex. For example, the  $^1\text{H}$  NMR spectrum of  $[\text{PhTt}^{\text{Ad}}]\text{NiCl}$  exhibited paramagnetically-shifted resonances, consistent with its  $S = 1$  ground state electronic structure, at  $\delta$  14.1, 7.8 and 7.2 compared with the values of 19.1, 7.7 and 7.1 for  $[\text{PhTt}^{\text{Bu}}]\text{NiCl}$ .<sup>18</sup>

We reported<sup>20</sup> that methyl lithium is a convenient, albeit uncommon, reductant for the generation of the nickel(i) complexes,  $[\text{PhTt}^{\text{Bu}}]\text{Ni}(\text{L})$ ,  $\text{L} = \text{CO}$ ,  $\text{PMe}_3$ ,  $\text{CNBu}'$ .<sup>21</sup> With regard to isolated yields, this reagent effects the transformation better than sodium borohydride, sodium amalgam and other alkyl lithium reagents. Mechanistic studies were in accord with an electron transfer role for methyl lithium with no evidence for a methylnickel intermediate in the reaction path. The complexes  $[\text{PhTt}^{\text{Ad}}]\text{Ni}(\text{L})$ ,  $\text{L} = \text{CO}$ ,  $\text{PMe}_3$ , were synthesized in moderate yields *via* an analogous route, Scheme 3.

In a typical reaction, the donor ligand ( $\text{CO}$  or  $\text{PMe}_3$ ) was added to solution at low temperatures prior to introduction of methyl lithium. The yellow nickel(i) species,  $[\text{PhTt}^{\text{Ad}}]\text{Ni}(\text{L})$ , are



Scheme 3

thermally stable and soluble in low polarity solvents. The complexes degrade rapidly upon exposure to protic solvents or dioxygen (*vide supra*). The  $^1\text{H}$  NMR spectra of the  $[\text{PhTt}^{\text{Ad}}]\text{Ni}(\text{L})$  complexes exhibit paramagnetically-shifted resonances in agreement with their magnetic moments,  $[\text{PhTt}^{\text{Ad}}]\text{Ni}(\text{CO})$ ,  $\mu_{\text{eff}} = 1.8 \mu_{\text{B}}$  and  $[\text{PhTt}^{\text{Ad}}]\text{Ni}(\text{PMe}_3)$ ,  $\mu_{\text{eff}} = 2.1 \mu_{\text{B}}$ , deduced by solution methods. The spectra indicate three-fold symmetric coordination of the borato ligand even at lower temperatures,  $-50^\circ\text{C}$ . The protons of the methylene carbon attached to boron in the  $[\text{PhTt}^{\text{Ad}}]$  ligand are most influenced by the paramagnetism of the complexes with shifts of *ca.* 84 to 114 ppm relative to the chemical shifts of the ligand. Given these observations, the ESR spectral characteristics of the complexes (anisotropic, axial signals), and the nature of the ligands, the complexes are assigned the nickel(i) formalism with little unpaired spin density on the ligands. That the replacement of the *tert*-butyl substituents for 1-adamantyl groups in the borato ligands is of no consequence to the electronic structure of the resulting metal complexes is highlighted by similarity of the  $\nu(\text{CO})$  modes of  $[\text{PhTt}^{\text{Ad}}]\text{Ni}(\text{CO})$  ( $1997 \text{ cm}^{-1}$ ) and  $[\text{PhTt}^{\text{Bu}}]\text{Ni}(\text{CO})$  ( $1999 \text{ cm}^{-1}$ ). Despite the congruent electronic properties, the  $[\text{PhTt}^{\text{Ad}}]$  and  $[\text{PhTt}^{\text{Bu}}]$  ligands impart different steric properties, as noted in the subtle differences in their structural parameters (detailed below) and in the strikingly different reactivity of the nickel(i) complexes with dioxygen.

Reduction of  $[\text{PhTt}^{\text{Ad}}]\text{NiCl}$  by methyl lithium in the absence of a suitable trapping ligand yielded an orange–brown diamagnetic solid in low yield, Scheme 3. The assignment of the product as the thiametallacycle,  $[\kappa^2\text{-PhTt}^{\text{Ad}}]\text{Ni}(\eta^2\text{-CH}_2\text{SAd})$ , was indicated by its NMR and UV-visible spectral properties and corroborated by X-ray diffraction analysis. The thiametallacycle arises presumably from the alkylation of a  $[\text{PhTt}^{\text{Ad}}]\text{Ni}^{\text{I}}$  fragment by excess  $[\text{PhTt}^{\text{Ad}}]^-$  generated in solution during the reduction. In fact, addition of  $[\text{PhTt}^{\text{Ad}}]\text{Ti}$  to  $[\text{PhTt}^{\text{Ad}}]\text{NiCl}$  produced the thiametallacycle in moderate yield. A similar mechanism was proposed for the formation of the related thiametallacycles,  $[\kappa^2\text{-PhTt}^{\text{Bu}}]\text{Ni}(\eta^2\text{-CH}_2\text{SBu}')$ <sup>20</sup> and  $[\text{Ph}_2\text{Bt}^{\text{Bu}}]\text{Ni}(\eta^2\text{-CH}_2\text{SBu}')$ .<sup>22</sup> Consistent with this overall reaction scheme, the presence of a suitable donor ligand ( $\text{CO}$  or  $\text{PMe}_3$ ) results in interception of the  $[\text{PhTt}^{\text{R}}]\text{Ni}^{\text{I}}$  fragment prior to alkylation by the borato ligand in solution.

### Molecular structures

The solid state structures of  $[\text{PhTt}^{\text{Ad}}]\text{Ni}(\text{CO})$ ,  $[\text{PhTt}^{\text{Ad}}]\text{Ni}(\text{PMe}_3)$  and  $[\kappa^2\text{-PhTt}^{\text{Ad}}]\text{Ni}(\eta^2\text{-CH}_2\text{SAd})$  are depicted in Figs. 1 and 2, with selected metric parameters and crystallographic data contained in Tables 1 and 3, respectively. Each molecule forms a discrete molecular entity in the solid state with a structure consistent with that assigned based on NMR spectral analyses.  $[\text{PhTt}^{\text{Ad}}]\text{Ni}(\text{CO})$  and  $[\text{PhTt}^{\text{Ad}}]\text{Ni}(\text{PMe}_3)$  are approximately three-fold symmetric with the monodentate donors residing on a (non-crystallographically imposed) three-fold axis. As always observed for this class of ligands when bound in the  $\kappa^3$  mode, the sulfur substituents are canted in the same direction so as to reduce unfavorable steric interactions.<sup>18</sup> As the structures of the related *tert*-butyl substituted complexes were reported earlier,

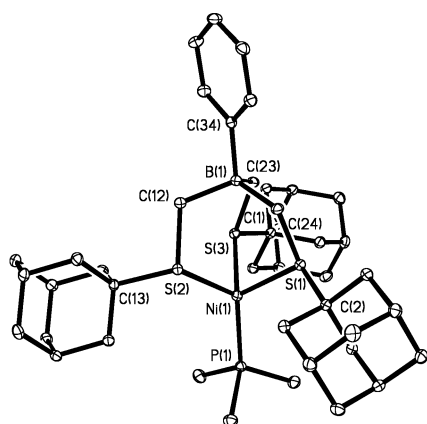
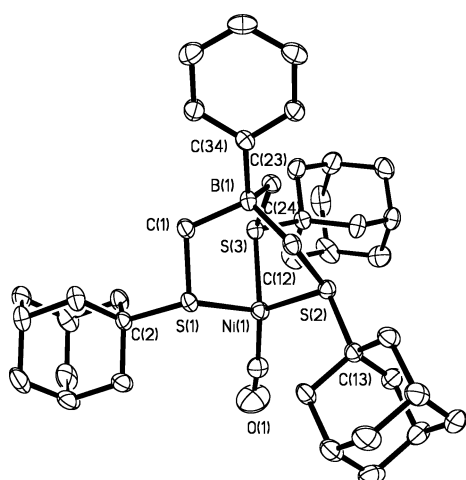


**Fig. 1** Thermal ellipsoid plots of  $[\text{PhTt}^{\text{Ad}}]\text{Ni}(\text{CO})$  (top) and  $[\text{PhTt}^{\text{Ad}}]\text{Ni}(\text{PMe}_3)$  (bottom) at the 30% probability level. Hydrogen atoms not shown.

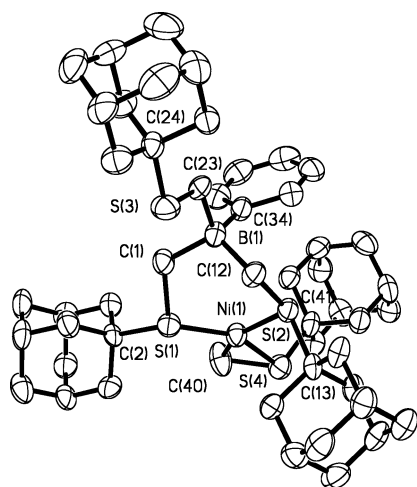


**Fig. 2** Thermal ellipsoid plots of  $[\kappa^2\text{-PhTt}^{\text{Ad}}]\text{Ni}(\eta^2\text{-CH}_2\text{SAd})$  at the 30% probability level. Hydrogen atoms not shown.

the present results provide the opportunity to compare these structures directly.

Careful examination of the related structures, Table 2, reveals that for the series of three complexes, no systematic trend is evident. The average Ni–S distance of 2.269(2) Å in  $[\text{PhTt}^{\text{Ad}}]\text{Ni}(\text{CO})$  is longer than the 2.238(3) Å bond length observed in  $[\text{PhTt}^{\text{Bu}}]\text{Ni}(\text{CO})$ . In contrast, the  $[\text{PhTt}^{\text{R}}]\text{Ni}(\text{PMe}_3)$  complexes exhibit the opposite ordering, *i.e.* the Ni–S distances are longer in  $[\text{PhTt}^{\text{Bu}}]\text{Ni}(\text{PMe}_3)$  than in  $[\text{PhTt}^{\text{Ad}}]\text{Ni}(\text{PMe}_3)$ . Nonetheless, the 1-adamantyl substituent is effective at precluding bimolecular complex formation under conditions in which  $[\text{PhTt}^{\text{Bu}}]$ -supported complexes lead to dinuclear species.<sup>23</sup>

**Table 1** Selected metric parameters (Å, °) for  $[\text{PhTt}^{\text{Ad}}]\text{Ni}(\text{CO})$ ,  $[\text{PhTt}^{\text{Ad}}]\text{Ni}(\text{PMe}_3)$  and  $[\kappa^2\text{-PhTt}^{\text{Ad}}]\text{Ni}(\eta^2\text{-CH}_2\text{SAd})$

$[\text{PhTt}^{\text{Ad}}]\text{Ni}(\text{CO})$			
Ni(1)–C(40)	1.815(4)	Ni(1)–S(2)	2.273(1)
Ni(1)–S(1)	2.263(1)	Ni(1)–S(3)	2.270(1)
C(40)–Ni(1)–S(1)	115.8(1)	S(1)–Ni(1)–S(2)	95.19(4)
C(40)–Ni(1)–S(3)	120.7(1)	S(3)–Ni(1)–S(2)	94.88(3)
S(1)–Ni(1)–S(3)	97.09(3)	O(1)–C(40)–Ni(1)	175.0(4)
C(40)–Ni(1)–S(2)	126.7(1)		
$[\text{PhTt}^{\text{Ad}}]\text{Ni}(\text{PMe}_3)$			
Ni(1)–P(1)	2.1941(5)	Ni(1)–S(2)	2.2829(5)
Ni(1)–S(1)	2.2835(4)	Ni(1)–S(3)	2.2801(5)
P(1)–Ni(1)–S(3)	119.99(2)	P(1)–Ni(1)–S(1)	120.63(2)
P(1)–Ni(1)–S(2)	124.43(2)	S(3)–Ni(1)–S(1)	93.52(2)
S(3)–Ni(1)–S(2)	96.88(2)	S(2)–Ni(1)–S(1)	94.22(2)
$[\kappa^2\text{-PhTt}^{\text{Ad}}]\text{Ni}(\eta^2\text{-CH}_2\text{SAd})$			
Ni(1)–C(40)	1.956(9)	Ni(1)–S(4)	2.150(2)
Ni(1)–S(1)	2.168(2)	S(4)–C(40)	1.742(8)
Ni(1)–S(2)	2.242(2)		
C(40)–Ni(1)–S(4)	49.9(2)	S(4)–Ni(1)–S(2)	105.97(9)
C(40)–Ni(1)–S(1)	108.0(2)	S(1)–Ni(1)–S(2)	96.54(9)
S(4)–Ni(1)–S(1)	154.46(9)	C(40)–S(4)–Ni(1)	59.2(3)
C(40)–Ni(1)–S(2)	155.5(2)	C(41)–S(4)–Ni(1)	112.8(3)

**Table 2** Comparative Ni–L bond distances (Å) for the complexes  $[\text{PhTt}^{\text{R}}]\text{Ni}(\text{CO})$ ,  $[\text{PhTt}^{\text{R}}]\text{Ni}(\text{PMe}_3)$  and  $[\kappa^2\text{-PhTt}^{\text{R}}]\text{Ni}(\eta^2\text{-CH}_2\text{SR})$ , R = *tert*-butyl or 1-adamantyl

	Ni–S <sub>av</sub>	Ni–L
$[\text{PhTt}^{\text{Bu}}]\text{Ni}(\text{PMe}_3)$	2.298	2.212(1)
$[\text{PhTt}^{\text{Ad}}]\text{Ni}(\text{PMe}_3)$	2.281	2.194(1)
$[\text{PhTt}^{\text{Bu}}]\text{Ni}(\text{CO})$	2.238	1.754(7)
$[\text{PhTt}^{\text{Ad}}]\text{Ni}(\text{CO})$	2.269	1.815(4)
$[\kappa^2\text{-PhTt}^{\text{Bu}}]\text{Ni}(\eta^2\text{-CH}_2\text{SBu}^t)$	2.176	1.939(5) Ni–C; 2.256(1) Ni–S
$[\kappa^2\text{-PhTt}^{\text{Ad}}]\text{Ni}(\eta^2\text{-CH}_2\text{SAd})$	2.159	1.956(9) Ni–C; 2.242(2) Ni–S

## Conclusions

The ligand  $[\text{PhTt}^{\text{Ad}}]$ , which possesses 1-adamantyl groups on the thioethers, was prepared readily from 1-bromoadamantane following the protocol developed for this class of ligands. From this new ligand four nickel complexes have been synthesized including two nickel(II) species designed to effect the reductive activation of dioxygen. Comparison of the appropriate spectroscopic and structural parameters for  $[\text{PhTt}^{\text{Ad}}]\text{Ni}(\text{L})$  with those reported previously for  $[\text{PhTt}^{\text{Bu}}]\text{Ni}(\text{L})$  indicates that the 1-adamantyl for *tert*-butyl replacement yields a ligand that imparts identical electronic properties with greater steric requirements. Specifically, the  $[\text{PhTt}^{\text{Ad}}]$  ligand provides the necessary steric impediment to prevent dimer formation. For example, reaction of  $[\text{PhTt}^{\text{Ad}}]\text{Ni}(\text{CO})$  with dioxygen yields a mononuclear, thermally sensitive O<sub>2</sub>-adduct that is the subject of a separate report.<sup>23</sup> This monomer contrasts with the purple dimer,  $[(\text{PhTt}^{\text{Bu}})\text{Ni}]_2(\mu\text{-O})_2$ , generated by a similar reaction.

## Experimental

### General considerations

Preparation of the nickel complexes was conducted either in an inert atmosphere glovebox or on a Schlenk line. Diethyl ether, THF and pentanes were freshly distilled over Na/benzophenone. Methanol was distilled over Mg ribbon. TMEDA was distilled over CaH<sub>2</sub>. 1-Adamantane thiol and 1-adamantane methyl sulfide were prepared according to the literature procedures.<sup>14</sup> Other reagents were used as received from com-

**Table 3** Crystallographic data for [PhTt<sup>Ad</sup>]Ni(CO), [PhTt<sup>Ad</sup>]Ni(PMe<sub>3</sub>), [κ<sup>2</sup>-PhTt<sup>Ad</sup>]Ni(η<sup>2</sup>-CH<sub>2</sub>SAd) and [PhTt<sup>Ad</sup>]Ti

Compound	[PhTt <sup>Ad</sup> ]Ni(CO)·CH <sub>3</sub> CN	[PhTt <sup>Ad</sup> ]Ni(PMe <sub>3</sub> )·THF·0.5C <sub>5</sub> H <sub>12</sub>	[κ <sup>2</sup> -PhTt <sup>Ad</sup> ]Ni(η <sup>2</sup> -CH <sub>2</sub> SAd)·(CH <sub>3</sub> ) <sub>2</sub> CO	[PhTt <sup>Ad</sup> ]Ti·2.5CHCl <sub>3</sub>
Formula	C <sub>42</sub> H <sub>59</sub> BNNiOS <sub>3</sub>	C <sub>48.5</sub> H <sub>79</sub> BNiOPS <sub>3</sub>	C <sub>53</sub> H <sub>79</sub> BNiOS <sub>4</sub>	C <sub>41.5</sub> H <sub>58.5</sub> BTiS <sub>3</sub> Cl <sub>7.5</sub>
Formula mass/g mol <sup>-1</sup>	759.60	874.79	929.92	1134.62
Temperature/K	223(2)	100(2)	223(2)	173(2)
Crystal system	Monoclinic	Monoclinic	Triclinic	Triclinic
Space group	<i>P</i> 2(1)/ <i>n</i>	<i>P</i> 2(1)/ <i>n</i>	<i>P</i> $\bar{1}$	<i>P</i> $\bar{1}$
<i>a</i> /Å	13.917(4)	15.062(2)	13.198(4)	13.3263(18)
<i>b</i> /Å	11.629(3)	19.580(2)	13.392(4)	16.333(2)
<i>c</i> /Å	23.722(7)	15.653(2)	15.607(5)	23.039(3)
<i>α</i> /°	90	90	88.952(7)	74.611(2)
<i>β</i> /°	94.156(6)	93.736(2)	66.668(6)	89.092(2)
<i>γ</i> /°	90	90	80.078(6)	75.496(2)
Volume/Å <sup>3</sup>	3829(2)	4606(1)	2491(1)	4673.8(11)
<i>Z</i>	4	4	2	4
Absorption coefficient/mm <sup>-1</sup>	0.705	0.627	0.594	4.048
Total reflections	27934	28794	15874	45397
Independent reflections	9290 [R(int) = 0.0630]	10739 [R(int) = 0.0194]	9626 [R(int) = 0.0779]	16418 [R(int) = 0.0294]
Final <i>R</i> indices [ <i>I</i> > 2σ( <i>I</i> )]	0.0623	0.0369	0.0903	0.0522
	0.1513	0.1181	0.2139	0.1419
<i>R</i> indices (all data)	0.0986	0.0416	0.1880	0.0637
	0.1738	0.1233	0.2587	0.1509

Wavelength, 0.71073 Å.

mercial vendors. Elemental analyses were performed by Desert Analytics, Inc. NMR spectra were recorded on a Bruker AM250, AC250 or DRX400 spectrometer. Chemical shifts ( $\delta$ ) were referenced to residual proton in the deuterated solvent for <sup>1</sup>H and <sup>13</sup>C NMR spectra and vs. external 85% H<sub>3</sub>PO<sub>4</sub> for <sup>31</sup>P spectra. FT-IR spectra were recorded on an Mattson Genesis series spectrometer. UV-Vis spectra were recorded on a HP 8453 diode array spectrophotometer.

### Synthesis

**[PhTt<sup>Ad</sup>]Ti.** 1-Adamantane methyl sulfide (14.8 g, 81 mmol) and TMEDA (12.3 mL, 81 mmol) were added to a 500 mL round-bottom flask that was vented through an aqueous solution of NaOCl under a N<sub>2</sub> atmosphere. Bu<sup>n</sup>Li (33 mL, 2.5 M in hexanes) was added dropwise *via* syringe over a period of 10 minutes. As the Bu<sup>n</sup>Li was added the reaction mixture became yellow and heterogeneous. Consequently, Et<sub>2</sub>O (100 mL) was added to facilitate stirring. After stirring for 24 hours at ambient temperature, PhBCl<sub>2</sub> (3.5 mL, 27 mmol) was added *via* syringe at -78 °C. The mixture was stirred for an additional 24 hours. The reaction was terminated by addition of methanol (25 mL). The volatiles were removed under vacuum. The yellow solid was dissolved in CHCl<sub>3</sub> (200 mL). After filtration the solvent was removed under vacuum. The resulting viscous oil was dissolved in acetone (200 mL) and water (50 mL), and treated with Ti<sub>2</sub>SO<sub>4</sub> (14.0 g, 28 mmol). The resulting pale green solid was collected and dissolved in CHCl<sub>3</sub> (200 mL). After filtering through Celite, the solvent was removed and the off-white solid was washed with Et<sub>2</sub>O. Yield 10.1 g (44%, 12 mmol). Crystals suitable for X-ray diffraction study were obtained with recrystallisation from CHCl<sub>3</sub>-hexane. <sup>1</sup>H NMR (CDCl<sub>3</sub>):  $\delta$  7.54 [(*o*-C<sub>6</sub>H<sub>5</sub>)B, br, 2 H], 7.40 [(*m*-C<sub>6</sub>H<sub>5</sub>)B, t, 2 H], 7.19 [(*p*-C<sub>6</sub>H<sub>5</sub>)B, t, 1 H], 2.38 (BCH<sub>2</sub>, d, 3 H), 2.06 (BCH<sub>2</sub> and C<sub>10</sub>H<sub>15</sub>S, br, 9 H), 1.90 (C<sub>10</sub>H<sub>15</sub>S, d, 12 H), 1.85 (C<sub>10</sub>H<sub>15</sub>S, d, 12 H), 1.69 (C<sub>10</sub>H<sub>15</sub>S, br, 15 H). <sup>13</sup>C NMR (CDCl<sub>3</sub>):  $\delta$  133.2 [(*o*-C<sub>6</sub>H<sub>5</sub>)B], 129.2 [(*p*-C<sub>6</sub>H<sub>5</sub>)B], 125.4 [(*m*-C<sub>6</sub>H<sub>5</sub>)B], 45.8 (C<sub>10</sub>H<sub>15</sub>S), 43.4 (C<sub>10</sub>H<sub>15</sub>S), 36.3 (C<sub>10</sub>H<sub>15</sub>S), 29.7 (C<sub>10</sub>H<sub>15</sub>S), 23.3 (CH<sub>2</sub>B), not observed [(*ipso*-C<sub>6</sub>H<sub>5</sub>)B]. Due to variable amounts of CHCl<sub>3</sub> solvation of solid samples, satisfactory combustion analysis has not been obtained.

**[PhTt<sup>Ad</sup>]NiCl.** [PhTt<sup>Ad</sup>]Ti (3.24 g, 3.88 mmol) in CHCl<sub>3</sub> (100 mL) was added dropwise to NiCl<sub>2</sub>·6H<sub>2</sub>O (0.92 g, 3.87 mmol) in methanol (50 mL) to form a red solution and a white

precipitate. The volatiles were removed under vacuum, yielding a reddish-brown solid. The solid was dissolved in CH<sub>2</sub>Cl<sub>2</sub> (100 mL), and filtered through Celite. After the solvent was removed under vacuum, the solid was extracted with CHCl<sub>3</sub> (3 × 100 mL). The volatiles were removed and [PhTt<sup>Ad</sup>]NiCl was washed with pentanes. Yield 1.35 g (48%, 1.85 mmol). <sup>1</sup>H NMR (CDCl<sub>3</sub>):  $\delta$  14.1 (br, C<sub>10</sub>H<sub>15</sub>S), 7.8 (br, C<sub>6</sub>H<sub>5</sub>B), 7.2 (br, C<sub>6</sub>H<sub>5</sub>B), 2.2 (br, C<sub>10</sub>H<sub>15</sub>S), 1.6 (br, C<sub>10</sub>H<sub>15</sub>S), -2.6 (br, C<sub>10</sub>H<sub>15</sub>S). UV-Vis (CH<sub>2</sub>Cl<sub>2</sub>),  $\lambda_{\max}$ /nm ( $\epsilon$ /M<sup>-1</sup> cm<sup>-1</sup>): 290 (1620), 393 (1510), 432 (1450), 536 (120), 841 (90). Anal. calc. for C<sub>39</sub>H<sub>56</sub>BCINiS<sub>3</sub>: C, 64.5; H, 7.77. Found: C, 64.7; H, 7.93%.

**[PhTt<sup>Ad</sup>]Ni(CO).** [PhTt<sup>Ad</sup>]NiCl (184 mg, 0.25 mmol) was dissolved in 100 mL of THF and the solution was kept at -78 °C in a dry ice-acetone bath. CO was bubbled through the red solution at -78 °C for about 5 minutes, and CH<sub>3</sub>Li (0.24 mL of a 1.6 M Et<sub>2</sub>O solution, 0.38 mL) was added slowly *via* syringe. The reaction mixture turned from red to orange with concomitant formation of a white solid. The solution was warmed to ambient temperature under an atmosphere of CO with stirring continued for 10 h. The solvent was removed under vacuum, and the resulting residue was extracted with Et<sub>2</sub>O then eluted through a plug of silica gel. The volatiles were removed yielding a yellow solid. [PhTt<sup>Ad</sup>]Ni(CO) was purified by recrystallisation from THF-pentane. Yield 52 mg (29%, 0.07 mmol). Crystals suitable for X-ray analysis were obtained by crystallisation from THF-acetonitrile-Et<sub>2</sub>O at -40 °C. <sup>1</sup>H NMR (toluene-*d*<sub>8</sub>):  $\delta$  116.3 (CH<sub>2</sub>B, br), 13.7 (br, C<sub>6</sub>H<sub>5</sub>B), 8.6 (br, C<sub>6</sub>H<sub>5</sub>B), -1.3 (d, C<sub>10</sub>H<sub>15</sub>S), -1.5 (d, C<sub>10</sub>H<sub>15</sub>S), -8.7 (br, C<sub>10</sub>H<sub>15</sub>S). FT-IR (KBr)  $\nu_{\text{CO}}$ : 1997 cm<sup>-1</sup>. UV-Vis (toluene),  $\lambda_{\max}$ /nm ( $\epsilon$ /M<sup>-1</sup> cm<sup>-1</sup>): 304 (2680), 348 (1900), 439 (1530).  $\mu_{\text{eff}}$  = 1.81  $\mu_{\text{B}}$  in C<sub>6</sub>H<sub>6</sub>. Anal. calc. for C<sub>54</sub>H<sub>72</sub>OS<sub>3</sub>BNi ([PhTt<sup>Ad</sup>]Ni(CO)·2toluene): C, 71.8; H, 8.04. Found: C, 72.0; H, 8.61%.

**[PhTt<sup>Ad</sup>]Ni(PMe<sub>3</sub>).** [PhTt<sup>Ad</sup>]NiCl (189 mg, 0.26 mmol) was dissolved in 100 mL of THF and the solution was kept at -78 °C in a dry ice-acetone bath. PMe<sub>3</sub> (0.26 mL of a 1.0 M THF solution, 0.26 mmol) was added to the solution *via* syringe generating a purple solution. CH<sub>3</sub>Li (0.24 mL of a 1.6 M Et<sub>2</sub>O solution, 0.38 mmol) was added slowly to the purple solution resulting in a rapid color change to yellow. The solution was warmed to ambient temperature with stirring continued for 10 h during which a white solid precipitated. The solvent was removed under vacuum, and the resulting residue was extracted with Et<sub>2</sub>O, eluted through a plug of silica gel. The volatiles were

removed yielding [PhTt<sup>Ad</sup>]Ni(PMe<sub>3</sub>) as a pale yellow solid, 97 mg (46%, 0.13 mmol). Crystals suitable for X-ray analysis were obtained by crystallisation from THF–pentanes at –40 °C. <sup>1</sup>H NMR (toluene-d<sub>8</sub>): δ 86.0 (br, CH<sub>2</sub>B), 22.8 [br, P(CH<sub>3</sub>)<sub>3</sub>], 17.7 (br, C<sub>6</sub>H<sub>5</sub>B), 10.4 (br, C<sub>6</sub>H<sub>5</sub>B), –0.3 (s, C<sub>10</sub>H<sub>15</sub>S), –1.9 (d, C<sub>10</sub>H<sub>15</sub>S), –2.5 (d, C<sub>10</sub>H<sub>15</sub>S), –12.8 (br, C<sub>10</sub>H<sub>15</sub>S). <sup>31</sup>P NMR (benzene-d<sub>6</sub>): δ 272. UV-Vis (toluene), λ<sub>max</sub>/nm (ε/M<sup>–1</sup> cm<sup>–1</sup>): 342 (1840), 443 (590). μ<sub>eff</sub> = 2.05 μ<sub>B</sub> in C<sub>6</sub>H<sub>6</sub>. Anal. calc. for C<sub>42</sub>H<sub>65</sub>PS<sub>3</sub>BNi: C, 65.8; H, 8.55. Found: C, 66.1; H, 8.95%.

[κ<sup>2</sup>-PhTt<sup>Ad</sup>]Ni(η<sup>2</sup>-CH<sub>2</sub>SAd). CH<sub>3</sub>Li (0.11 mL of a 1.6 M Et<sub>2</sub>O solution, 0.18 mmol) was added dropwise to a THF (100 mL) solution of [PhTt<sup>Ad</sup>]NiCl (100 mg, 0.14 mmol) at –78 °C. A dark brown solid precipitated as the solution was warmed to ambient temperature. The solvent was removed and the residue dissolved in Et<sub>2</sub>O, followed by elution through a plug of silica gel. The volatiles were removed to yield an orange solid, 6 mg (5%, 0.007 mmol). <sup>1</sup>H NMR (toluene-d<sub>8</sub>): δ 7.94 [(*o*-C<sub>6</sub>H<sub>5</sub>)B, d, 2 H], 7.39 [(*m*-C<sub>6</sub>H<sub>5</sub>)B, t, 2 H], 7.14 [(*p*-C<sub>6</sub>H<sub>5</sub>)B, d, 1 H], 2.3 (CH<sub>2</sub>B, br, 6 H), 2.04 (C<sub>10</sub>H<sub>15</sub>S, br, 16 H), 1.90 (C<sub>10</sub>H<sub>15</sub>S, br, 8 H), 1.79 [Ni(η<sup>2</sup>-CH<sub>2</sub>SC<sub>10</sub>H<sub>15</sub>), d, 1 H], 1.75 (C<sub>10</sub>H<sub>15</sub>S, br, 2 H), 1.64 (C<sub>10</sub>H<sub>15</sub>S, br, 2 H), 1.61 (C<sub>10</sub>H<sub>15</sub>S, br, 3 H), 1.54 (C<sub>10</sub>H<sub>15</sub>S, br, 14 H), 1.50 (C<sub>10</sub>H<sub>15</sub>S, 3 H), 1.37 (C<sub>10</sub>H<sub>15</sub>S, br, 4 H), 1.26 (C<sub>10</sub>H<sub>15</sub>S, m, 4 H), 1.21 [Ni(η<sup>2</sup>-CH<sub>2</sub>SC<sub>10</sub>H<sub>15</sub>), d, 1 H], 0.89 (C<sub>10</sub>H<sub>15</sub>S, d, 2 H), 0.87 (C<sub>10</sub>H<sub>15</sub>S, d, 2 H). UV-Vis (toluene), λ<sub>max</sub>/nm (ε/M<sup>–1</sup> cm<sup>–1</sup>): 336 (680), 362 (200), 474 (260), 1067 (81). Anal. calc. for C<sub>50</sub>H<sub>73</sub>S<sub>4</sub>BNi: C, 68.9; H, 8.44. Found: C, 68.3; H, 8.44%.

### X-Ray crystallography

Crystallographic data were collected on a Bruker-AXS SMART APEX-CCD system with graphite-monochromated Mo-Kα radiation. A suitable crystal was mounted on a glass fiber under perfluoropolyether. Crystal, data collection, and refinement parameters are given in Table 3. For the crystals of [PhTt<sup>Ad</sup>]Ni(CO) and [PhTt<sup>Ad</sup>]Ni(PMe<sub>3</sub>) the systematic absences in the diffraction data are uniquely consistent with the space group *P2*(1)/*n*. For the crystals of [PhTt<sup>Ad</sup>]Ti and [κ<sup>2</sup>-PhTt<sup>Ad</sup>]Ni(η<sup>2</sup>-CH<sub>2</sub>SAd) *E*-statistics and the value of *Z* suggested the centrosymmetric space group option, *P* $\bar{1}$ , which yielded chemically reasonable and computationally stable results of refinement. The structures were solved using direct methods, completed by subsequent difference Fourier syntheses, and refined by full-matrix least-squares procedures. Absorption corrections were applied to the data using SADABS.<sup>24</sup> All non-hydrogen atoms were refined with anisotropic displacement coefficients.

CCDC reference numbers 199593–199596.

See <http://www.rsc.org/suppdata/dt/b2/b212271e/> for crystallographic data in CIF or other electronic format.

### Acknowledgements

We thank the National Science Foundation (CHE-9974628 and CHE-0213260) for support of this work.

### References

- 1 K. Nag and A. Chakravorty, *Coord. Chem. Rev.*, 1980, **33**, 87–147.
- 2 M. A. Halcrow and G. Christou, *Chem. Rev.*, 1994, **94**, 2421–2481.
- 3 B. S. Mandimutsira, J. L. Yamarik, T. C. Brunold, W. Gu, S. P. Cramer and C. G. Riordan, *J. Am. Chem. Soc.*, 2001, **123**, 9194–9195.
- 4 L. Que and W. B. Tolman, *Angew. Chem., Int. Ed.*, 2002, **41**, 1114–1137.
- 5 R. Schenker, B. S. Mandimutsira, C. G. Riordan and T. C. Brunold, *J. Am. Chem. Soc.*, 2002, **124**, 13842–13855.
- 6 S. Hikichi, M. Yoshizawa, Y. Sasakura, H. Komatsuzaki, Y. Moro-oka and M. Akita, *Chem. Eur. J.*, 2001, **7**, 5011–5028.
- 7 S. Hikichi, M. Yoshizawa, Y. Sasakura, M. Akita and Y. Moro-oka, *J. Am. Chem. Soc.*, 1998, **120**, 10567–10568.
- 8 K. Shiren, S. Ogo, S. Fujinami, H. Hayashi, M. Suzuki, A. Uehara, Y. Watanabe and Y. Moro-oka, *J. Am. Chem. Soc.*, 2000, **122**, 254–262.
- 9 S. Itoh, H. Bandoh, M. Nakagawa, S. Nagatomo, T. Kitagawa, K. D. Karlin and S. Fukuzumi, *J. Am. Chem. Soc.*, 2001, **123**, 11168–11178.
- 10 H. C. Liang, M. Dahan and K. D. Karlin, *Curr. Opin. Chem. Biol.*, 1999, **3**, 168–175.
- 11 K. D. Karlin, S. Kaderli and A. D. Zuberbuhler, *Acc. Chem. Res.*, 1997, **30**, 139–147.
- 12 W. B. Tolman, *Acc. Chem. Res.*, 1997, **30**, 227–237.
- 13 V. Mahadevan, M. J. Henson, E. I. Solomon and T. D. P. Stack, *J. Am. Chem. Soc.*, 2000, **122**, 10249–10250.
- 14 K. K. Khullar and L. Bauer, *J. Org. Chem.*, 1971, **36**, 3038–3040.
- 15 A. I. Vogel and D. M. Cowan, *J. Chem. Soc.*, 1943, 18.
- 16 S.-J. Chiou, J. Innocent, K.-C. Lam, C. G. Riordan, L. Liable-Sands and A. L. Rheingold, *Inorg. Chem.*, 2000, **39**, 4347–4353.
- 17 C. Ohrenberg, P. Ge, P. Schebler, C. G. Riordan, G. P. A. Yap and A. L. Rheingold, *Inorg. Chem.*, 1996, **35**, 749–754.
- 18 P. J. Schebler, C. G. Riordan, I. Guzei and A. L. Rheingold, *Inorg. Chem.*, 1998, **37**, 4754–4755.
- 19 C. Ohrenberg, C. G. Riordan, L. M. Liable-Sands and A. L. Rheingold, *Inorg. Chem.*, 2001, **40**, 4276–4283.
- 20 P. J. Schebler, B. S. Mandimutsira, C. G. Riordan, L. Liable-Sands, C. D. Incarvito and A. L. Rheingold, *J. Am. Chem. Soc.*, 2001, **123**, 331–332.
- 21 P. L. Holland, T. R. Cundari, L. L. Perez, N. A. Eckert and R. J. Lachicotte, *J. Am. Chem. Soc.*, 2002, **124**, 14416–14424.
- 22 P. H. Ge, A. L. Rheingold and C. G. Riordan, *Inorg. Chem.*, 2002, **41**, 1383–1390.
- 23 K. Fujita and C. G. Riordan, manuscript in preparation.
- 24 G. M. Sheldrick, SADABS, Program for area detector adsorption correction, Institute for Inorganic Chemistry, University of Göttingen, Germany, 1996.